RSC Advances

PAPER

View Article Online
View Journal | View Issue

Check for updates

Cite this: *RSC Adv.*, 2025, **15**, 312

Photo-crosslinked Diels–Alder and thiol–ene polymer networks†

Masa Alrefai and Milan Maric *

Compositions of ethylene glycol dicyclopentenyl ether methacrylate (EGDEMA), a vegetable oil based alkyl methacrylate (C13MA), and furfuryl methacrylate (FMA) were terpolymerized for dual-crosslinked networks with tailored mechanical and thermal properties. Specifically, initiators for continuous activator regeneration (ICAR) atom transfer radical polymerization (ATRP) afforded materials with tailored glass transition temperature (T_g) and incorporation of furan and norbornene functionalities within a single chain. The terpolymer with high furan and norbornene functionality (Ter2: $F_{FMA} = 0.42$, $F_{EGDEMA} = 0.46$, $F_{C13MA} = 0.12$) is crosslinked to form single-crosslinked reversible networks with 1,1′-(methylenedi-4,1-phenylene)bismaleimide (BM) *via* Diels–Alder (DA) chemistry and dual-crosslinked networks incorporating additional non-reversible thiol–ene crosslinks. The reactions were photo-initiated using 254 nm UV light with BM : FMA molar ratios of 0.1 and 0.2 for both systems. FTIR analyses for crosslinked Ter2 samples confirmed the successful formation of DA and thiol–ene adducts, while DSC confirmed the reversibility of the DA reaction. A terpolymer with higher C13MA composition (Ter3: $F_{C13MA} = 0.75$, $F_{FMA} = 0.17$, $F_{EGDEMA} = 0.08$) was similarly crosslinked in single and dual crosslinked networks with BM : FMA of 0.1 and 0.2. Crosslinking efficiency was evaluated for both single and dual crosslinked networks with a BM : FMA = 0.1 by comparing thermal and UV curing methods, with UV curing proving more effective for dual-crosslinked systems, leading to increased gel content (71% with UV compared to 61% thermally) and improved material properties. FTIR and DSC results confirmed the formation of the DA adducts and the reversibility of the DA reaction. The terpolymers were further analyzed for adhesive applications through rheological testing. These studies demonstrated that the incorporation of thiol–ene crosslinking alongside Diels–Alder crosslinking offers a balanced combination of reversible and permanent bonds, resulting in materials with enhanced mechanical strength, thermal stability, and functional versatility that are suitable for applications such as recyclable adhesives.

Received 13th November 2024
Accepted 23rd December 2024

DOI: 10.1039/d4ra08072f

rsc.li/rsc-advances

Open Access Article. Published on 03 January 2025. Downloaded on 7/19/2025 8:17:25 PM.
This article is licensed under a Creative Commons Attribution-NonCommercial 3.0 Unported Licence.

Introduction

The growing concerns over fossil resource depletion, environmental impacts, and price volatility have spurred interest in alternative sustainable materials.[1] Polymeric adhesives that are bio-sourced and reusable, recyclable, and self-healing offer sustainable alternatives by reducing waste and conserving resources. These materials extend product lifespans, improve reliability, and minimize waste.[2]

Dynamic covalent bonds, such as those formed through the Diels–Alder (DA) reaction, provide reversible properties to polymer networks, allowing them to respond to external stimuli.[3] The DA reaction, involving a [4 + 2] cycloaddition between a diene and a dienophile, is temperature-controlled and suitable for recyclable and self-healing materials as it undergoes the reversible reaction (r-DA) upon heating.[4–6] However, fully reversible polymer networks may lose mechanical robustness at elevated temperatures.[7] Interpenetrating polymer networks (IPNs) that combine irreversible and reversible crosslinks can maintain the polymer networks' mechanical strength and structural integrity over a wide temperature range.[7] Click reactions, including DA and thiol–ene, are effective post-polymerization modification and crosslinking methods. They can be initiated photochemically or thermally; however, photo-initiation coupling is particularly efficient, offering faster reaction times and lower energy requirements compared to thermal initiation.[1] To address the challenge of maintaining mechanical robustness in fully reversible polymer networks, dual crosslinked networks that combine Diels–Alder with thiol–ene chemistry offer an effective solution by incorporating both reversible and irreversible crosslinks. Thiol–ene click chemistry is a highly efficient method for polymerization, curing, and modification.[8] It involves a rapid, step-wise reaction between thiol and "ene" groups.[9] Key benefits include fast

Dept. of Chemical Engineering, McGill University, 3610 Rue Universite, Montreal, QC H3A 0C5, Canada. E-mail: milan.maric@mcgill.ca

† Electronic supplementary information (ESI) available. See DOI: https://doi.org/10.1039/d4ra08072f

© 2025 The Author(s). Published by the Royal Society of Chemistry

Open Access Article. Published on 03 January 2025. Downloaded on 7/19/2025 8:17:25 PM. This article is licensed under a Creative Commons Attribution-NonCommercial 3.0 Unported Licence.

reaction rates, minimal shrinkage, and high tolerance to oxygen.[9,10]

To enable a dual crosslinking system, it is necessary to synthesize polymers with dual functionalities. This can be achieved by copolymerizing functional monomers like furfuryl methacrylate (FMA) and ethylene glycol dicyclopentenyl ether methacrylate (EGDEMA),[11] which introduce furan and norbornene functional groups, respectively, to the polymer. Traditional free radical polymerization can be challenging for these functional monomers due to potential side reactions leading to gelation.[12] Therefore, advanced controlled radical polymerization methods are employed; one such method is Atom Transfer Radical Polymerization (ATRP).[13–15] ATRP enables the synthesis of polymers with precise molecular weights, tailored architectures, and narrow molecular weight distributions, making it highly versatile for various applications.[16] However, a significant drawback of traditional ATRP is the high concentration of catalysts, typically copper, which pose an environmental hazard.[17] Therefore, low-catalyst ATRP methods were developed to address this environmental concern. One such method is initiators for continuous activator regeneration (ICAR) ATRP.[18] ICAR ATRP utilizes a low concentration of organic free radicals for controlled polymerization with minimal catalyst, providing greater stability but potentially broader molecular weight distributions.[19,20] Our previous work featured the synthesis of poly(FMA) using the low catalyst ATRP method, ICAR, and the subsequent crosslinking with photo-DA click reaction.[21] Incorporating bio-sourced monomers like FMA, derived from cellulosic biomass, not only adds functionality, allowing post-polymerization modification of the furan bond with DA click chemistry, but also contributes to the sustainability of these materials.[4] The other functionality, imparted from EGDEMA units with the norbornene cyclic hydrocarbon, facilitates thiol–ene click chemistry reactions with thiols.[22] Our previous work featured the controlled polymer synthesis of EGDEMA by traditional ATRP and ARGET ATRP;[23] however, to the best of our knowledge, ICAR ATRP of EGDEMA has not yet been reported.

Based on our previous work on DA cross-linked self-healing polymer networks,[18] further efforts can be directed into investigating this crosslinking chemistry with other crosslinking chemistries for applications such as adhesive formulation. Incorporating thiol–ene crosslinking in addition to Diels–Alder crosslinking provides a balanced combination of reversible and permanent bonds, leading to a material with enhanced mechanical strength, thermal stability, chemical resistance, and functional versatility. This dual-crosslinking approach allows for the development of robust materials with tailored properties suitable for a wide range of applications, including self-healing materials, smart coatings, and high-performance adhesives.

Experimental methods

Materials

Furfuryl methacrylate (FMA, 97%) was purchased from Millipore Sigma; a mixture of alkyl methacrylates with an average chain length of 13 carbons (C13MA, >99%) and isobornyl methacrylate (IBOMA ≥ 99%) were obtained from Evonik. Ethylene glycol dicyclopentenyl ether methacrylate (EGDEMA ≥ 90%) was purchased from Millipore Sigma. The monomers were purified by passing through a column of basic alumina (Brockmann, Type 1, 150 mesh, Sigma-Aldrich) mixed with 5 wt% calcium hydride (90–95% reagent grade, Sigma-Aldrich) to remove the inhibitor and then stored in a sealed round bottom flask under a head of nitrogen in a refrigerator until needed. Ethyl α-bromoisobutyrate (EBiB 98%), copper(II) bromide ($CuBr_2$ 99%), 1,1′-(methylenedi-4,1-phenylene) bismaleimide (BM), and anisole (99%) were all obtained from Sigma-Aldrich and used as received. Ethylene bis(3-mercaptopropionate), Thiocure® 320 (TC), was obtained from Bruno Bock Chemische Fabrik GmbH & Co, and used as received. 2,2-Dimethoxy-2-phenylacetophenone (DMPA, ≥99%) was obtained from Aldrich and used as received. Toluene (≥99%), tetrahydrofuran (THF, 99.9% HPLC grade), methanol (MeOH, ≥99%), and the ligand tris(2-dimethylaminoethyl) amine (Me6TREN, +98%) were obtained from Fisher Scientific and used as received. The deuterated chloroform ($CDCl_3$, ≥99%) used as a solvent for proton nuclear magnetic resonance (^{1}H NMR) was purchased from Cambridge Isotopes Laboratory.

Synthesis methods

Synthesis of poly (EGDEMA) and poly(FMA-*co*-EGDEMA-*co*-C13MA) by ICAR ATRP. ICAR ATRP was utilized for synthesizing homopolymers and terpolymers of EGDEMA, FMA, and C13MA. The terpolymers' composition is shown in Table 1. For the typical synthesis of poly(EGDEMA), a 100 mL round-bottom three-necked flask was used. Initially, 6.8 mg (0.03 mmol) of $CuBr_2$ and 0.02 g (0.1 mmol) of the ligand Me_6TREN were added to the flask and stirred under a nitrogen purge for 20 minutes. Subsequently, 6.6 g (40 mmol) of the monomer FMA in a 50 wt% anisole solution (6.6 g of anisole) and 0.04 g (0.2 mmol) of AIBN were introduced. At the designated temperature, 0.12 g (0.62 mmol) of the initiator EBiB was added. The target number average degree of polymerization (DP_n) for these reaction was 100, corresponding to a molecular weight of $M_{n,target}$ = 22.3 kg mol^{-1} at complete conversion for homopoly(EGDEMA). The reactor was fitted with a condenser in the middle neck and maintained at 3 °C to prevent the evaporation of the monomer or solvent. A magnetic stir bar was placed in the reactor, which was set on a heating mantle atop a stirrer. The mixture was continuously purged with nitrogen throughout the polymerization. The mixture was then heated at a rate of 3 °C min^{-1}, with

Table 1 Experimental conditions for ICAR ATRP terpolymerizations of EGDEMA, FMA, and C13MA[a]

	F_{FMA}	F_{C13MA}	F_{EGDEMA}	M_n target (kg mol^{-1})
Ter1	0.3	0.4	0.3	22.5
Ter2	0.4	0.2	0.4	21.4
Ter3	0.2	0.7	0.1	23.8

[a] The experimental setup for ICAR ATRP was [monomer]:[EBiB]:[Cu(II)] = 100:1:0.05 [Cu(II)]:[Me_6TREN] = 1:2, and [AIBN]:[EBiB] = 0.4 at 70 °C in 50 wt% anisole solution.

Open Access Article. Published on 03 January 2025. Downloaded on 7/19/2025 8:17:25 PM. This article is licensed under a Creative Commons Attribution-NonCommercial 3.0 Unported Licence.

the nitrogen purge vented through the condenser *via* a needle inserted into a septum. Polymerization was initiated once the temperature reached 70 °C, monitored by a thermocouple in the left neck of the flask. The reaction was terminated when the mixture became excessively viscous, making it impossible to take further samples. At this point, the heating was turned off, and the reactor was allowed to cool. The resulting polymers were precipitated in excess methanol; the supernatant was decanted and dried in the fume hood.

Synthesis of dual-crosslinked thermo-reversible network polymer *via* furan-maleimide Diels–Alder and thiol–ene click reactions. The polymers were dissolved in a 50 wt% solution of toluene and mixed with 1,1′-(methylenedi-4,1-phenylene) bismaleimide (BM), and ethylene bis(3-mercaptopropionate), Thiocure® 320 (TC), for the dual-crosslinked samples, as well as the photo-initiator DMPA. The photo-initiator was used at a 4% loading compared to the polymer. The samples were then poured into aluminum plates and irradiated at 254 nm for 10 minutes. The samples were then left in the fumehood overnight to dry. The terpolymer prepared Ter2: ($F_{C13MA} = 0.12$, $F_{FMA} = 0.42$, and $F_{EGDEMA} = 0.6$) was crosslinked in a single crosslinked network with DA only by adding two different loadings of the bismaleimide crosslinker (BM) to form T2A and T2C and in a dual crosslinked system of DA and thiol–ene with the addition of both BM and the di-thiol TC to form T2B and T2D. Ter3 ($F_{C13MA} = 0.75$, $F_{FMA} = 0.17$, and $F_{EGDEMA} = 0.08$) was crosslinked similarly, and all the samples prepared are shown in Table 2 below. Thermally crosslinked Ter3 samples were cured at a temperature of 120 °C in a vacuum oven.

Polymer characterization

Thermogravimetric analysis and differential scanning calorimetry. The T_g of the polymers was estimated using a DSC Discovery 2500 from TA Instruments. The T_g measurements were conducted under a nitrogen atmosphere at a heating/cooling rate of 15 °C min^{-1} with three scans per cycle (heat/cool/heat). The T_g values were determined by the inflection point method on DSC traces obtained from the second heating run. Additionally, thermogravimetric analysis (TGA) was performed using a Discovery 5500 TGA (TA Instruments) to assess the thermal stability of the polymers. The TGA analysis was carried out with a temperature ramp rate of 20 °C min^{-1}, ranging from 25 °C to 600 °C under a nitrogen atmosphere.

Fourier-transform infrared spectroscopy (FTIR). Monitoring of the furan, norbornene, thiol, and maleimide functional groups was done using FTIR from dried samples. A Thermo Scientific Nicolet IS50-ATR FTIR spectrophotometer equipped with an attenuated total reflectance (ATR) diamond attachment was used, with 32 scans per spectra. The signal was normalized to a constant peak at 2900 cm^{-1}, corresponding to the C–H bond, which does not react, to account for the differences in concentrations of different samples.

Polymer swelling test. To verify the crosslinking of the polymers, the synthesized polymers were immersed in THF, where they exhibited swelling. The swollen polymer samples were then dried and weighed to determine the gel content. The reported values are the average of two measurements.

^{1}H NMR spectroscopy. ^{1}H NMR analysis was performed using a Varian NMR Mercury spectrometer with 300 MHz and 16 scans using deuterated chloroform ($CDCl_3$) as a solvent. ^{1}H NMR data of Ter3 (δ, ppm): 7.36–7.48 (m, H, –CH=CH–, FMA monomer), 6.12–6.16 and 5.58–5.60 (m, 1H, –CH=CH–, EGDEMA monomer) & 6.05–6.12 and 5.51–5.56 (d, 2H, –CH_2–CH=C–, C13MA monomer), 4.80–5.15 (s, 2H, O–CH_2–C=, FMA polymer), 4.06–4.17, (s, 2H, O–CH_2–C=, EGDEMA polymer), 3.8–4.09 (m, 2H, –CH_2–, C13MA polymer). The ^{1}H NMR traces of the homopolymer and terpolymer of EGDEMA are shown in the ESI in Fig. S1 and S2.†

Rheology. Rheological testing of the polymer samples was performed using an Anton Paar MCR 302 Rheometer. To determine the viscoelastic properties of the samples, the rheometer was used to perform an amplitude sweep (shear strain = 0.01–1%) to determine the viscoelastic region, and in dynamic mechanical analysis (DMA) mode while using a parallel plate geometry to observe structural transitions (25 mm, at 1 mm gap). The DMA tests were performed with a temperature ramp from room temperature up to 120 °C (frequency = 1 Hz, normal force $F_N = 1$ N, and shear strain 0.1%). As for the frequency sweep test, the angular frequency was varied from 0.1–100 rad s^{-1} with an amplitude of 1% of the material thickness. Measurements were taken at room temperature. The storage and loss moduli (G' and G'') were reported at a shear rate of 1 s^{-1} and an angular frequency of 1 rad

Table 2 Experimental conditions for crosslinked terpolymer samples: terpolymer crosslinked by single (DA) and dual (DA & thiol–ene) networks

Polymer	Ter2[d]				Ter3[e]					
Crosslinking system	Single	Dual	Single	Dual	Single	Dual	Single	Dual	Single	Dual
Curing method	UV[f]	UV[f]	UV[f]	UV[f]	UV[f]	UV[f]	Thermal[g]	Thermal[g]	UV[f]	UV[f]
Crosslinked samples[a]	T2A	T2B	T2C	T2D	T3A	T3B	T3AT	T3BT	T3E	T3F
BM : FMA[b]	0.1	0.1	0.2	0.2	0.1	0.1	0.1	0.1	0.2	0.2
TC : EGDEMA[c]	0	0.1	0	0.1	0	0.4	0	0.4	0	0.4

[a] T2A-D samples are the crosslinked formulations derived from Ter2, whereas T3A-F samples are the crosslinked formulations derived from Ter3. [b] The molar ratio of the bismaleimide crosslinker (BM groups to FMA in the terpolymer to form DA crosslinks). [c] The molar ratio of the thiol crosslinker (TC) groups to EGDEMA in the terpolymer to form thiol–ene crosslinks. [d] Ter2: $F_{C13MA} = 0.12$, $F_{FMA} = 0.42$, and $F_{EGDEMA} = 0.6$. [e] Ter3: $F_{C13MA} = 0.75$, $F_{FMA} = 0.17$, and $F_{EGDEMA} = 0.08$. [f] UV curing was performed by irradiating the at 254 nm for 10 minutes. [g] Thermal curing was done by heating the samples to 120 °C.

© 2025 The Author(s). Published by the Royal Society of Chemistry

Open Access Article. Published on 03 January 2025. Downloaded on 7/19/2025 8:17:25 PM. This article is licensed under a Creative Commons Attribution-NonCommercial 3.0 Unported Licence.

s^{-1}, respectively, for comparable values within the viscoelastic region. In addition, tack tests were performed on the samples using the parallel plate geometry; in the experiment, the upper plate geometry was lifted at a constant velocity of 500 μm s^{-1}, and the force was monitored as a function of displacement (gap).

Results & discussion

Homopolymer synthesis of poly(EGDEMA) by ICAR ATRP

ICAR ATRP was employed to synthesize homopolymers of poly(EGDEMA). ATRP methods are tolerant to various functional groups, enabling the synthesis of functional polymer chains with minimum gelation.[13–15] ICAR ATRP, is a low-catalyst ATRP method, that requires only ppm amounts of catalyst, therefore eliminating the need for post-polymerization treatment for the removal of catalyst presenting a more environmentally friendly controlled synthesis method. The reactions were conducted in a 50 wt% solution of anisole, with AIBN serving as the initiator for the reduction of the copper catalyst and EBiB acting as the ATRP initiator. The reaction was maintained at a temperature of 70 °C, and samples were collected throughout to monitor the kinetics. Our previous work on the controlled polymerization of EGDEMA using the low-catalyst ATRP method ARGET ATRP reported dispersity ($Đ$) of 1.38 for homopolymers of EGDEMA and 1.38–1.76 for copolymers of EGDEMA and C13MA.[23] The primary disadvantage of the reported ARGET ATRP is the use of tin hexanoate $Sn(EH)_2$ as a reducing agent. Although $Sn(EH)_2$ is FDA approved, its reduction produces Sn(IV), which is more toxic than $Sn(EH)_2$.[24] In contrast, ICAR ATRP avoids this issue by using a traditional free radical initiator as the reducing agent. However, this initiator generates new chains, which can impact the properties of the copolymer.[18,25] The results from ICAR ATRP of EGDEMA showed higher $Đ = 1.46–1.59$ than what is typically associated with ATRP; the higher $Đ$ could be attributed to radical termination due to side reactions of the functional norbornene group and/or free-radical polymerization initiated by AIBN.[25] Table 3 summarizes the EGDEMA homopolymers prepared *via* ICAR ATRP EG1 And EG2, with two number average degrees of polymerization (DP_n) of 50 and 100, respectively. The polymerization was well controlled, as indicated by the M_n increasing linearly along the predicted line in the M_n *versus* conversion graph as well as the linear semi-logarithmic plot of scaled conversion with time kinetic plot shown in Fig. 1. The GPC trace shows a monomodal, relatively narrow peak; the trace of EG2 is shown in Fig. 1.

Terpolymer synthesis by ICAR ATRP

Terpolymers of norbornene functional EGDEMA and furan functional FMA, along with the bio-based methacrylic monomer C13MA, were prepared using ICAR ATRP. A controlled radical polymerization method, such as ICAR ATRP, allows the synthesis of functional polymers with pre-determined molecular weights and permits better chain-to-chain compositional homogeneity.[19] However, copolymerization and

Table 3 Characterization of poly(EGDEMA) homopolymers synthesized *via* ICAR ATRP with varying DP_n

	[Monomer] : [EBiB] : [Cu(II)]	$M_{n,target}$ (kg mol^{-1})	M_n[a] (kg mol^{-1})	X[b] (%)	$Đ$[a]
EG1[c]	50 : 1 : 0.03	11	10	41	1.46
EG2[c]	100 : 1 : 0.03	22	18	64	1.59

[a] The final product's number average molecular weight (M_n) and dispersity ($Đ$) as estimated by GPC relative to PMMA standards at 40 °C in THF. [b] The conversion (X) was determined by ^{1}H NMR. [c] ICAR ATRP reaction conditions were [I] : [EBiB] = 0.4, Cu(II) : Me_6TREN = 1 : 2 carried out at 70 °C in 50 wt% anisole solution.

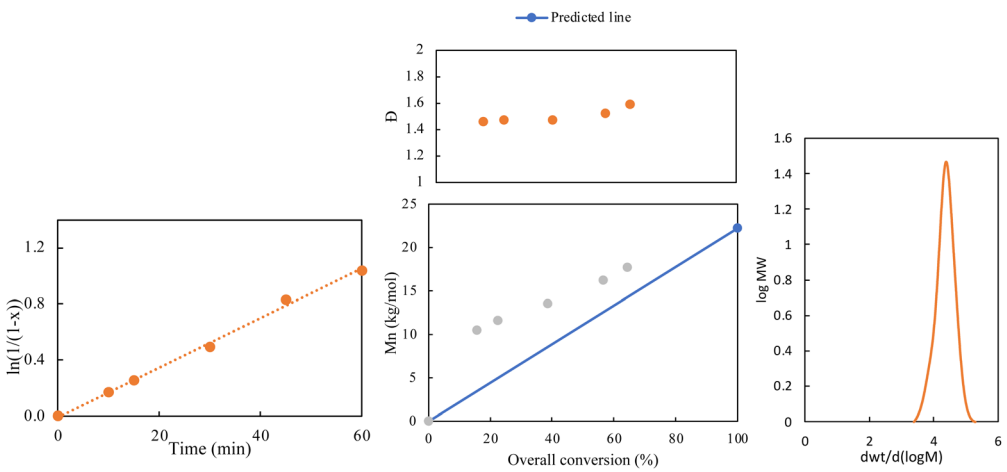

Fig. 1 Kinetic results of the homopolymerization of EGDEMA by ICAR ATRP (EG2) with [monomer] : [EBiB] : [Cu(II)] = 100 : 1 : 0.03 [Cu(II)] : [Me_6TREN] = 1 : 2, and [AIBN] : [EBiB] = 0.4.

Open Access Article. Published on 03 January 2025. Downloaded on 7/19/2025 8:17:25 PM. This article is licensed under a Creative Commons Attribution-NonCommercial 3.0 Unported Licence.

terpolymerization using ICAR ATRP can be very challenging because the radical initiator can initiate new chains, leading to chain transfer and radical–radical termination.[18,25] Additionally, the dual functionality of the monomers poses a difficulty as the functional groups can participate in side reactions. Despite the challenges, we successfully synthesized furan-norbornene functional terpolymers using ICAR ATRP. Three different terpolymers were prepared, summarized in Table 4, with varying concentrations of functional groups. The resulting molecular weights were very close to the target values, and the dispersities ranged from $Đ = 1.59$ to 1.80, and $T_g = -27$ °C to −35 °C, depending on the terpolymer composition; the GPC traces are shown in Fig. S3.† The higher dispersity values can be attributed to possible side reactions by the functional groups and monomers undergoing free radical polymerization in the early stages of the reaction before proceeding through ICAR ATRP groups.[25] This is shown by the shoulder displayed on the right in the GPC traces, most apparent in Ter3 which had the highest dispersity of 1.80 and less prominent in Ter 2 which had a slightly lower dispersity of 1.65.

Synthesis of polymer networks *via* furan-maleimide and thiol–ene click reactions: comparison of DA network and dual crosslinked DA/thiol–ene networks

Our study investigates two crosslinking approaches: single crosslinking with DA and dual crosslinking combining DA with thiol–ene chemistries. The single crosslinking method relies on the thermal reversibility of DA bonds, which is beneficial for applications requiring temporary bonding or self-healing capabilities. However, the reversible DA bonds alone may not provide sufficient mechanical strength and stability, particularly at elevated temperatures, whereas dynamic fully reversible polymer networks can suffer from a loss of mechanical robustness and even structural integrity.[2,7] To address this limitation, the inclusion of a secondary crosslinking system of irreversible (static) crosslinks allows the material to retain its shape and preserve most of its mechanical properties.[2,7] Therefore, dual static and dynamic crosslinking networks were prepared by introducing irreversible static crosslinks (thiol–ene) to the reversible dynamic DA system, as shown in Scheme 1. Photo-cured dual crosslinked networks with DA and thiol–ene crosslinks have been reported by Wang *et al.*[26] In their study, a UV-curable self-healing coating was developed using a photo-click reaction between polyurethane acrylate containing Diels–Alder bonds and thiol monomers.[26] Our work, however, utilizes ICAR ATRP for the controlled synthesis of norbornene and furan functional polymers that are consequently crosslinked in one step with thiol and maleimide crosslinkers.

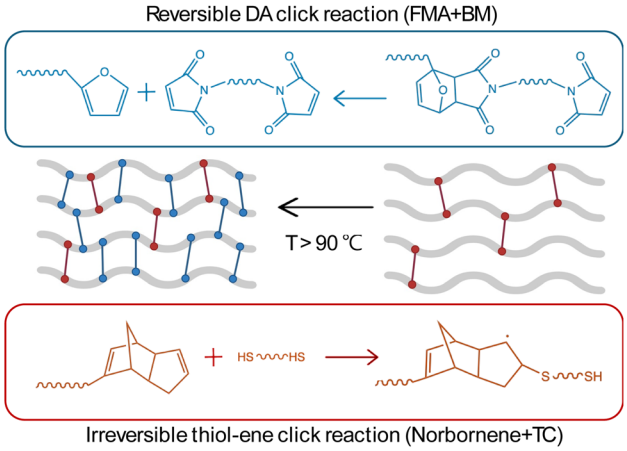

Scheme 1 Illustration of the dual crosslinked system of reversible DA crosslinks and permanent thiol–ene crosslinks.

The Ter2 polymer ($F_{C13MA} = 0.12$, $F_{FMA} = 0.42$, and $F_{EGDEMA} = 0.6$) was selected for the first part of this study due to its high content of cross-linkable functional groups. By utilizing a polymer with high functional group loading, the impact of the crosslinking strategies on the network's thermal stability and reversibility could be distinctly observed, making it an ideal candidate for evaluating the effects of single and dual crosslinking systems. The polymer was crosslinked using DA chemistry to form a single-crosslinked network (T2A, DA) and a combination of DA and thiol–ene chemistry to form a dual-crosslinked network (T2B, DA and thiol–ene). Additionally, the effect of increased BM : FMA loading (T2D, Dual, BM : FMA = 0.2) on the network properties was studied with a second dual-crosslinked system.

Initial characterization of crosslinked samples. FTIR studies were conducted to investigate the functional groups involved in the DA and thiol–ene reactions of the samples. The FTIR traces of the dual crosslinked sample of Ter 2 (T2B, DA and thiol–ene), normalized to the constant C–H peak at 2850 cm^{-1}, are presented in Fig. S4.† The dual-crosslinked sample T2B was chosen to confirm the formation of both the DA and thiol–ene adducts. A prominent sharp peak at 1770 cm^{-1}, specific to the furan/maleimide adduct,[27] significantly increases, confirming the

Table 4 Molecular characterization of EGDEMA/FMA/C13MA terpolymerization *via* ICAR ATRP

	F(FMA)[a]	F(C13MA)[a]	F(EGDEMA)[a]	M_n (kg mol^{-1})[b]	$Đ$[b]	T_g[c] (°C)
IC-Ter1[d]	0.39	0.39	0.21	19.4	1.59	−27
IC-Ter2[d]	0.42	0.12	0.46	23.6	1.65	−30
IC-Ter3[d]	0.17	0.75	0.08	23.3	1.80	−35

[a] The final molar fraction of monomers F in the terpolymer as determined by ^{1}H NMR in $CDCl_3$. [b] The final product's number average molecular weight (M_n) and dispersity ($Đ$) as estimated by GPC relative to PMMA standards at 40 °C in THF. [c] The T_g as determined from DSC analysis in the second heating cycle of a heat/cool/heat test. [d] The experimental setup for ICAR ATRP reactions was [monomer] : [EBiB] : [Cu(II)] = 100 : 1 : 0.05, [Cu(II)] : [Me6TREN] = 1 : 2, and [AIBN] : [EBiB] = 0.4 at 70 °C in 50 wt% anisole solution.

© 2025 The Author(s). Published by the Royal Society of Chemistry

Open Access Article. Published on 03 January 2025. Downloaded on 7/19/2025 8:17:25 PM.
This article is licensed under a Creative Commons Attribution-NonCommercial 3.0 Unported Licence.

formation of the desired DA adduct. The disappearance of the peaks at 695 cm^{-1} and 750 cm^{-1} corresponding to the maleimide ring deformation and the furan respectively, as well as the peaks at 3142 cm^{-1} and 3114 cm^{-1} which correspond to the stretching vibration of C–H in furan rings, indicate the reaction of the bismaleimide with furan.[27–29] The disappearance of the peak at 2620 cm^{-1} corresponding the thiol group and the prominent increase in the peak at 600 cm^{-1} corresponding to the thiol–ene adduct confirm the thiol–ene reaction occurred.[30] Furthermore, the disappearance of the peak at 1600 cm^{-1}, corresponding to the C=C bond in the furan and norbornene pendant groups, indicates the effective consumption of the double bonds during the DA and thiol–ene reactions. Both reactions, thiol–ene[31] and the DA[32] reactions are known to be regioselective, and the FTIR results confirmed both type of crosslinks are forming in the photo-cured system.

TGA was first carried out to check the decomposition behavior for T2A (DA) and T2B (DA and thiol–ene) to provide insights into the thermal stability of the two systems, highlighting the effect of incorporating thiol–ene crosslinks alongside Diels–Alder chemistry. The dual crosslinked samples were also compared at two different loadings of 0.1 and 0.2. The TGA results, shown in Fig. 2, show two transitions for the single crosslinked sample (T2A), whereas a single transition is observed in the dual crosslinked samples (T2B and T2D), suggesting a more homogeneous thermal decomposition behavior, which indicates that the dual-crosslinking strategy has led to a more uniform and possibly more stable material under thermal conditions. Moreover, the dual crosslinked sample (T2B) showed a delayed onset of decomposition compared to the single crosslinked system (T2A), indicating higher thermal stability. Like what was observed in the swelling tests, the increased BM loading did not impact the thermal behavior of the network and the network at both loadings (T2B and T2D) showed comparable results, with the higher BM loading showing slightly higher thermal stability due to lower fractional change in the sample mass during the TGA test.

In the reversible DA click reaction, the r-DA reaction occurs upon heating, causing furan-maleimide adducts to break and re-form with temperature changes.[4] DSC was used to study the thermal behavior of these dynamic polymer networks and monitor the DA and r-DA reactions; the results are presented in Fig. 3. During the first heating cycle, the cured samples showed endothermic peaks, indicating the r-DA reaction where furan-maleimide bonds were cleaved upon heating and partially reformed upon subsequent cooling.[33] In the dual-crosslinked samples (T2D shown in Fig. 3), the reversibility of the DA reaction is maintained, confirming their recyclability; this is evidenced by the presence of endotherms in the first and second heating runs, indicating the breaking and reformation of DA bonds upon cooling and heating.

Comparatively, the DA crosslinked sample, T2A, showed a broad endotherm in the range of 40–100 °C whereas the dual crosslinked sample, T2B, showed a later onset endotherm at around 110 °C. The endotherm observed in T2A suggests a lower degree of crosslinking, whereas the later onset endotherm associated with T2B indicates increased thermal stability and higher crosslinking density due to the additional thiol–ene crosslinks. Moreover, the wide endothermic peak observed in T2D indicates a higher degree of crosslinking and the endothermic peaks are observed in both heating cycles for T2D indicating its recyclability as the DA adducts re-form upon cooling and break again when heated in the second cycle. These observations indicate that the dual-crosslinking system resulted in a higher degree of crosslinking and that the dynamic polymer networks undergo reversible DA reactions and emphasize the potential to tailor material properties more effectively (*e.g.* make them repairable).

Studies of Ter2 crosslinked samples showed that dual-crosslinking provided enhanced thermal behavior. UV curing successfully activated both DA and thiol–ene reactions. Having established the success of both the single and dual crosslinking systems, this system is then studied for application in recyclable adhesives. To achieve this, a terpolymer with low T_g imparted by a higher C13MA incorporation and lower FMA and EGDEMA loadings is utilized to obtain thermosetting elastomers that have sufficient chain mobility and flow that allow them to be recycled and self-healed.

Optimization: synthesis of polymer networks *via* furan-maleimide and thiol–ene click reactions

Comparison of UV and thermal crosslinking. A lower functional group concentration reduces crosslinking density, facilitating chain mobility and reversible bond dynamics. This allows the network to maintain elasticity and enables the reformation of bonds during thermal cycling or mechanical stress, which is critical for achieving tunable and recyclable material properties. Therefore, for the next part of the study, the

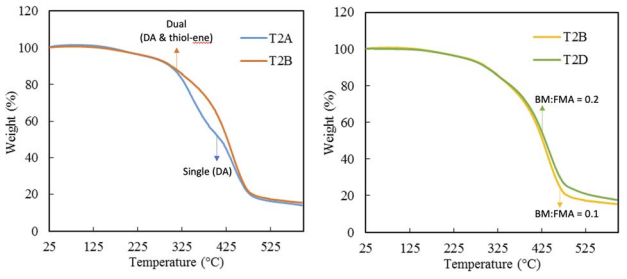

Fig. 2 TGA traces for crosslinked Ter2 samples with single crosslinking (T2A, BM : FMA = 0.1) and dual crosslinking (T2B, BM : FMA = 0.1; T2D, BM : FMA = 0.2).

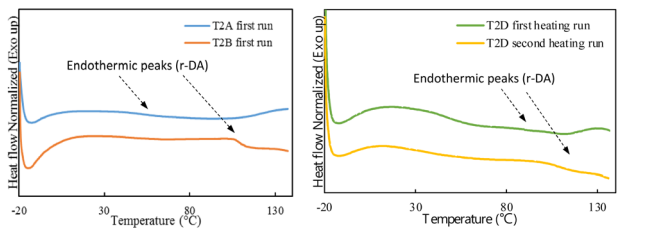

Fig. 3 DSC traces for crosslinked Ter2 samples with single and dual curing and BM : FMA loadings of 0.1 and 0.2 (T2A, T2B, and T2D).

Open Access Article. Published on 03 January 2025. Downloaded on 7/19/2025 8:17:25 PM. This article is licensed under a Creative Commons Attribution-NonCommercial 3.0 Unported Licence.

polymer with the lowest functional groups concentrations, terpolymer Ter3 (F_{C13MA} = 0.75, F_{FMA} = 0.17, and F_{EGDEMA} = 0.08) was crosslinked using both single (DA, T3A) and dual (DA & thiol–ene, T3B) crosslinking systems. First, optimization was done to evaluate the efficiency of UV curing relative to thermal curing for the crosslinked systems, UV-cured samples (T3A, DA and T3B, DA and thiol–ene) were compared to thermally cured samples (T3AT, DA and T3BT, DA and thiol–ene).

The FTIR traces for crosslinked Ter3 samples are presented in Fig. 4. Unlike the Ter2 cured samples, the peak at 1770 cm^{-1} specific to the furan/maleimide adduct does not show a clear increase since it overlaps with the C=O peak of C13MA that is in the terpolymer backbone.[27] However, for both UV- and thermally cured samples, evidence of crosslinking is shown through the significant decrease of the peak at 1600 cm^{-1} corresponding to the C=C bond in the furan and norbornene pendant groups, indicating the effective consumption of the double bonds during the DA reactions for both UV and thermally cured samples. Moreover, the disappearance of the peaks at 695 cm^{-1} and 750 cm^{-1} corresponding to the maleimide ring deformation and the furan, respectively, as well as the peaks at 3142 cm^{-1} and 3114 cm^{-1} correspond to the stretching vibration of C–H in furan rings, indicate the reaction of the bismaleimide and furan.[27–29] The FTIR results confirmed the formation of DA adducts both UV- and thermal cured samples.

Further analysis was done by performing swelling tests to examine the impact of crosslinking in both cases; the results are shown in Fig. 4. The gel content analysis shows that the dual crosslinked sample (T3B, DA and thiol–ene) has higher gel content compared to its counterpart with only DA crosslinks (T3A, DA), which indicates that the dual crosslinking leads to a more extensively crosslinked network. In contrast, when comparing the thermally cured to the UV cured samples for the dual crosslinked system, the thermally dual crosslinked sample T3BT exhibited lower gel content, which indicates less efficient thiol–ene crosslinking, which could be due to the thiol-maleimide reaction that can occur under thermal conditions.[34] The DA samples showed a higher gel content when thermally cured (T3AT) compared to the UV-cured sample (T3A), suggesting more efficient DA crosslinking. However, the lower gel content of T3BT indicates that the thermal curing is not efficient for a dual-crosslinked network of DA and thiol–ene. Therefore, in the context of a dual crosslinking system involving maleimide-furan and thiol-norbornene functionalities, UV

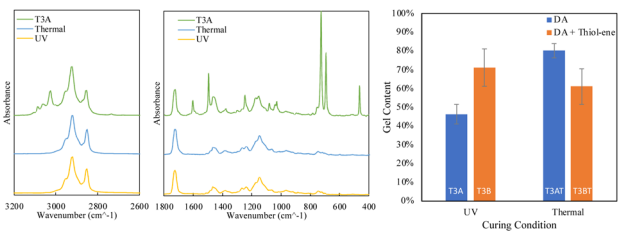

Fig. 4 FTIR traces for crosslinked Ter3 (F_{C13MA} = 0.75, F_{FMA} = 0.17, F_{EGDEMA} = 0.08) samples with single crosslinking using BM : FMA (Diels–Alder – DA) loading of 0.1 and gel content chart for UV and thermally cured samples.

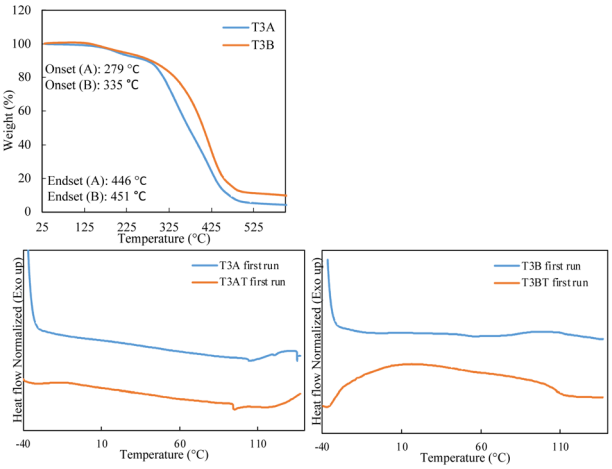

Fig. 5 Top: TGA traces of crosslinked Ter3 samples with single and dual crosslinking. Bottom: DSC traces for crosslinked Ter3 samples with single and dual curing and BM : FMA loadings of 0.1 showing UV-cured samples in comparison to thermally cured samples.

irradiation can be preferentially used to simultaneously activate the maleimide-furan DA reaction and the thiol-norbornene thiol–ene reaction while minimizing the thiol-Michael addition reaction between the thiol and bismaleimide crosslinkers.[34]

The TGA results, shown in Fig. 5, show that T3B (dual crosslinked) has a higher thermal stability compared to T3A (single crosslinked), with a higher onset temperature of 335 °C compared to 279 °C. Like that observed for the crosslinked Ter2 samples, a single transition is observed for the dual crosslinked samples, suggesting a more homogeneous thermal decomposition behavior. This indicates that the dual crosslinking in T3B (DA and thiol–ene) provides enhanced thermal resistance, likely due to the additional thiol–ene crosslinks that improve the overall network stability.

The DSC traces, shown in Fig. 5, show that T3A and T3AT have very similar traces, in which we see a broad endotherm in the range of 60–110 °C; this indicates the r-DA reaction taking place. While T3B shows an endothermic peak indicating an r-DA reaction taking place, T3BT shows a wide exothermic peak indicating a curing reaction taking place, which shows that during the thermal curing, the thiol–ene click reaction was inefficient; this agrees with the lower gel content observed.

Synthesis of polymer networks *via* furan-maleimide and thiol–ene click reactions for application as adhesives

Varying the BM loading. Having demonstrated the efficiency of UV curing for the dual-crosslinking system, we next investigated the adhesive performance of crosslinked Ter3 samples at varying BM : FMA loadings for both the single and dual crosslinked systems. Samples prepared for this test were at a higher BM loading (BM : FMA = 0.2, T3E and T3F) against a lower BM loading set (BM : FMA = 0.1, T3A and T3B) were prepared and UV-cured for comparison intended for use as adhesives. Swelling test results, shown in Fig. S5,† showed that the higher

© 2025 The Author(s). Published by the Royal Society of Chemistry

Open Access Article. Published on 03 January 2025. Downloaded on 7/19/2025 8:17:25 PM. This article is licensed under a Creative Commons Attribution-NonCommercial 3.0 Unported Licence.

BM loading resulted in higher gel content for T3E and T3F, indicating more densely crosslinked networks due to the additional crosslinks formed by the excess BM. Sample sets were studied rheologically, including DMA, frequency sweeps, and tack tests for the tacky samples.

The frequency sweep test shows storage modulus (G') and loss modulus (G'') for both samples increase with frequency, as shown in Fig. 6(a); G' is consistently higher than G'', indicating that the material is predominantly elastic. T3B exhibits lower G' and G'' compared to T3A across all frequencies of the network imparted by the flexibility of the thiol–ene crosslinks. This suggests that T3A has a stiffer and more elastic network. For adhesive applications, the frequency sweep tests can be used to characterize adhesives, as the low-frequency behavior is indicative of the shear strength of the adhesive, whereas the high-frequency behavior is indicative of the peel adhesion.[35] The frequency sweep results show promising adhesive behavior as they exhibit a decrease in modulus at low frequencies, which indicates favorable bonding, and an increase in modulus at high frequencies, which indicates stronger debonding.[36] Moreover, the storage moduli at room temperature at a frequency of 100 s^{-1} does not exceed 3 $\times$ 10^5, therefore they satisfy the Dahlquist criteria for pressure-sensitive adhesives.[37] Tack tests were conducted to evaluate the cohesive and adhesive properties of the formulations; the results are presented in Fig. 6(b). The maximum normal force observed during the tack test indicates the cohesive strength of the adhesive, while the area under the normal force–displacement curve represents the separation (dissipation) energy, which corresponds to the adhesive strength (tack). In the tack test, both T3A and T3B have a high initial normal force, indicating high cohesive strength imparted by the crosslinks, but T3B's lower initial normal force and more gradual decrease suggest that the thiol–ene crosslinks provide a more flexible and deformable network. For application in adhesives, the high initial normal force suggests that T3A can provide a strong initial adhesive bond, which is crucial for applications requiring immediate handling strength. The lower moduli and more gradual deformation indicate that T3B is more flexible and possesses higher tack.[38] Moreover, the gradual deformation in both formulations results in a greater area under the normal force *versus* displacement graph, thus implying high energy of separation and adhesive strength.[38] This flexibility can be advantageous in applications where the adhesive needs to accommodate thermal expansion, contraction, or mechanical stresses without failing.

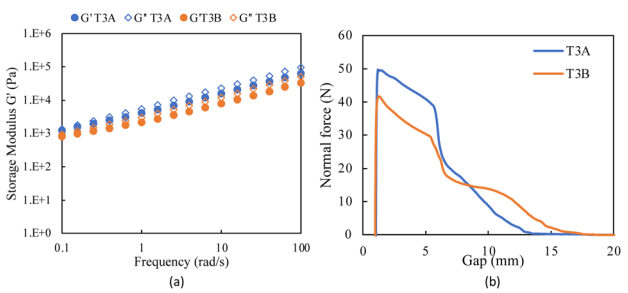

Fig. 6 Experimental results for rheological testing: frequency sweep (a) and tack test (b) results for UV-cured crosslinked Ter3 samples with single and dual crosslinking and a BM : FMA ratio of 0.1.

The DMA test results for T3A and T3B are shown in Fig. S6.† The results show that the G' for T3A decreases as temperature rises, reaching a minimum near 100 °C due to the retro-Diels–Alder (r-DA) reaction, where crosslinks break and the material softens.[39] T3B also exhibits a decrease in G', with a more pronounced drop around 90 °C, attributed to the flexibility of the additional thiol–ene crosslinks, which allow for greater polymer chain mobility (despite the extra crosslinking, the thiol bridge in the crosslinker is flexible). Both samples eventually lose their structural integrity at around 100 °C, transitioning into a viscous state and beginning to ooze out of plates.

The DMA results for T3E and T3F (Ter3 crosslinked with 0.2 BM (T3E) and 0.2 BM and 0.4 thiol:ene (T3F)) are shown in Fig. 7. In the DMA test results for T3E, G' gradually decreases over the temperature range 25 °C to about 100 °C and almost plateaus during the first heating cycle, indicating that the material becomes softer as the retro-Diels–Alder (r-DA) reaction occurs and the DA adducts break.[39] The presence of extra crosslinks allows the material to maintain its structural integrity, enabling the performance of a second heating cycle despite some loss of polymer as it transitioned into a viscous liquid state at a higher temperature, observed by the noise in the signal. In the second cycle, G' recovered with a slightly higher level than the first cycle, this can be attributed to the formation of additional DA crosslinks during heating, as the consecutive rapid heat-cool cycle performed may result in incomplete r-DA reaction, resulting in additional crosslinks.[40] The tan δ for T3E decreases steadily up to around 100 °C in the first cycle, reflecting a continuous loss of damping capability as the r-DA reaction progresses and the material transitions from a crosslinked to an un-crosslinked state.[41] In the second cycle, tan δ is lower across the temperature range compared to the first cycle, indicating reduced energy dissipation, possibly due to fewer reformed crosslinks. The noise observed at higher temperatures in both cycles corresponds to the polymer transitioning into a viscous liquid state, further confirming the impact of the retro-DA reaction on the material's structural integrity. This transition signifies that the network has lost its crosslinked structure, resulting in a complete loss of its solid-like behavior.[4]

For T3F, which is crosslinked with both DA and thiol–ene linkages, the samples retain their structural integrity, and no noise is observed in the signal. The G' of T3F samples decreases steadily with temperature in the first cycle, more so than in T3E, due to the flexibility provided by the additional thiol–ene crosslinks. This behavior shows that the material softens due to the r-DA reaction where crosslinks break. In the second cycle, G' is recovered and decreases, indicating that the network partially reformed and maintained a higher modulus than in the first cycle due to the formation of additional DA crosslinks during heating.[40] Tan δ for T3F shows a very slight decrease as some DA bonds break, but the loss factor remains relatively constant due to the thiol–ene crosslinks holding the network intact. After the initial decrease, tan δ slightly increases around 75 °C, indicating more complex thermal behavior due to the dual crosslinking, where the permanent thiol–ene crosslinks maintain the

Open Access Article. Published on 03 January 2025. Downloaded on 7/19/2025 8:17:25 PM.
This article is licensed under a Creative Commons Attribution-NonCommercial 3.0 Unported Licence.

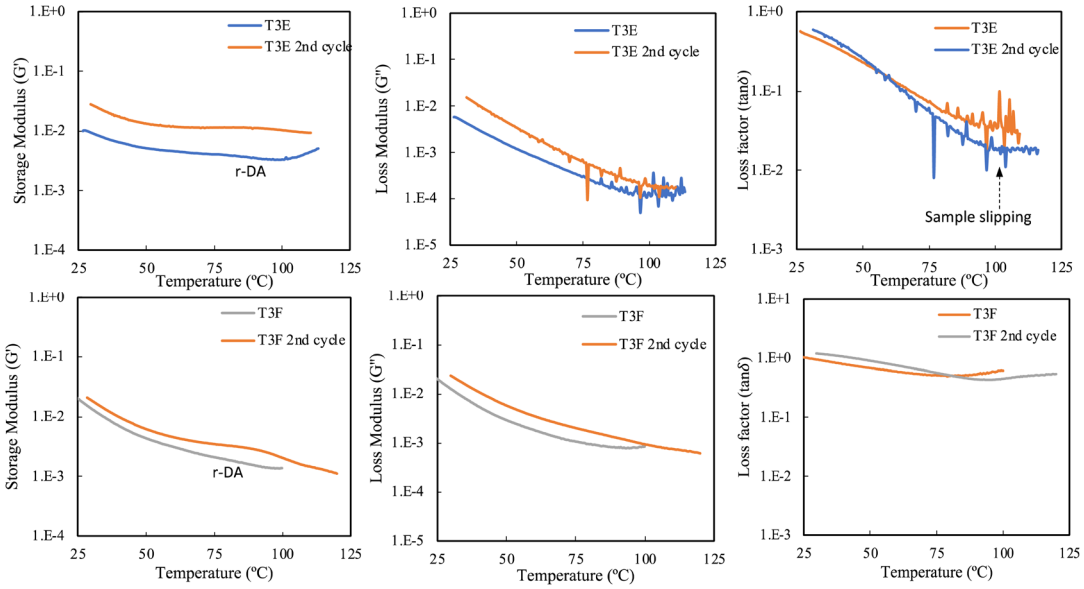

Fig. 7 DMA test results for two-cycle heating for single and dual crosslinked samples with BM : FMA ratio of 0.2; the reported units for G' and G'' are Pa.

structure as the DA bonds undergo the r-DA reaction; a similar pattern is observed in the second cycle. The dual-crosslinked networks demonstrate higher thermal stability and better retention of mechanical and damping properties across heating cycles compared to T3E samples, which only have DA crosslinking. Additionally, the observed transition from a crosslinked to an uncrosslinked state highlights the processing and reworkability of DA-crosslinked networks, allowing the material to be reshaped or recycled at elevated temperatures.[39] The ability to thermally cycle the samples and recover the storage modulus further indicates the material's recyclability.

The network characterization, thermal analysis, and rheological results suggest the dual crosslinking system offers improved thermal stability and flexibility, making it potentially more suitable for applications requiring both high thermal resistance and dynamic mechanical performance. This suggests that incorporating thiol–ene crosslinking results in a more resilient polymer network capable of maintaining its properties even after thermal cycling. The low T_g of these terpolymer samples enables chain mobility, while the reversible DA crosslinks enable recyclability and self-healing capabilities. Additionally, the thiol–ene crosslinks help maintain the structural integrity of the network. Together, these features make the dual-crosslinked networks an intriguing solution for recyclable adhesives.

Conclusions

This study successfully employed low-catalyst ICAR ATRP to synthesize homopolymers of EGDEMA, yielding colourless polymers with M_n near the target M_n with 10 kg mol^{-1} and 18 kg mol^{-1} for the DP_n of 50 and 100, respectively. The reaction was considered controlled based on M_n increasing linearly with conversion, maintaining relatively narrow, monomodal molecular weight distributions as well as linear semi-logarithmic kinetic plots. EGDEMA was terpolymerized using ICAR ATRP with bio-based methacrylates C13MA and FMA to tailor the T_g and introduce furan functionality. The resulting terpolymers were photo-crosslinked to form single-crosslinked reversible networks *via* DA chemistry and dual-crosslinked networks incorporating additional thiol–ene crosslinks.

The terpolymer Ter2 with a high and equal composition of functional groups for crosslinking (norbornene and furan) was crosslinked to study the difference between the single and dual-crosslinked networks as well as the effect of varying the BM crosslinker loading. FTIR analyses confirmed the formation of DA and thiol–ene adducts, whereas the DSC results showed endothermic peaks confirming the reversibility of the DA reaction. TGA measurements indicated a single T_g transition for dual-crosslinked systems, in contrast to the multiple transitions observed in single-crosslinked systems, suggesting a more uniform crosslinked network.

Next, the terpolymer Ter 3 with high C13MA content and a lower content of functional groups was crosslinked, as a looser network allows chain mobility and network flexibility for application in adhesives. Ter3 was crosslinked in single and dual crosslinked networks, with thermal and photo-chemical reactions compared (T3A, T3B, T3AT, and T3BT). FTIR results showed the adduct formation in both cases, but thermally crosslinked samples showed higher gel content for the single crosslinked network but lower gel content for the dual crosslinked network compared to the UV-cured samples; therefore, it was shown that UV curing proves to be more effective for dual-crosslinked systems, leading to improved material properties.

Ter3 was then studied for applicability towards recyclable adhesives; the terpolymer was crosslinked at BM : FMA loadings of 0.1 and 0.2 in single and dual crosslinked networks using UV light. Results showed that higher BM loading resulted in greater

© 2025 The Author(s). Published by the Royal Society of Chemistry

Open Access Article. Published on 03 January 2025. Downloaded on 7/19/2025 8:17:25 PM. This article is licensed under a Creative Commons Attribution-NonCommercial 3.0 Unported Licence.

gel content, indicative of more densely crosslinked networks. Rheological measurements of the crosslinked polymer networks of Ter3 showed that for all samples, DMA test results show the reversibility of the DA reaction as G' decreases upon heating, indicating the DA bonds break in an r-DA reaction. The dual-crosslinked networks, compared to those with only DA crosslinking, demonstrated superior thermal stability and better retention of mechanical and damping properties across two heating cycles. Furthermore, the ability to thermally cycle the samples and recover the elasticity highlights the material's re-processability and recyclability. The dual-crosslinking system in these functional terpolymers creates a matrix that enables a suite of tuneable, partially reversible networks suitable for recyclable adhesives.

Data availability

The data supporting this article have been included as part of the ESI.† Data for this article, including all raw data tabulated in Microsoft Excel or CSV format for DSC, TGA, GPC, Rheology, FTIR and ^{1}H NMR measurements are available at McGill University Dataverse [https://borealisdata.ca/dataverse/mcgill] at [https://borealisdata.ca/dataset.xhtml?persistentId=doi:10.5683/SP3/XOIUZQ].

Author contributions

Conceptualization: M. M. and M. A.; methodology: M. A.; validation: M. M. and M. A.; investigation: M. A.; resources: M. M.; data curation: M. A.; writing – original draft: M. A.; writing– review & editing: M. M. and M. A.; supervision: M. M.

Conflicts of interest

There are no conflicts to declare.

Acknowledgements

The authors would like to thank the Natural Sciences and Engineering Research Council of Canada (RGPIN-2024-04619) for funding and the NSERC CGS-D and the Vadasz Doctoral Fellowships (Faculty of Engineering, McGill University) for providing funding to M.A. The authors also thank Michael Schmidt and Tom Beyersdorff for facilitating the acquisition of the Thiocure® 320 from Bruno Bock Chemische Fabrik GmbH & Co. The authors also thank Jean Desroches from Thames River Chemicals Corp. (TRC) for facilitating the acquisition of the Terra Visiomer C13MA monomer from Evonik described in this work.

References

1 A. Vitale, G. Trusiano and R. Bongiovanni, *Rev. Adhes. Adhes.*, 2017, **5**, 105–161.
2 M. Zolghadr, A. Shakeri, M. J. Zohuriaan-Mehr and A. Salimi, *J. Appl. Polym. Sci.*, 2019, **136**, 48015.
3 J. Kötteritzsch, S. Stumpf, S. Hoeppener, J. Vitz, M. D. Hager and U. S. Schubert, *Macromol. Chem. Phys.*, 2013, **214**, 1636–1649.
4 A. Gandini, *Prog. Polym. Sci.*, 2013, **38**, 1–29.
5 E. E. L. Maassen, R. Anastasio, L. C. A. van Breemen, R. P. Sijbesma and J. P. A. Heuts, *Macromol. Chem. Phys.*, 2020, **221**, 1–7.
6 T. N. Gevrek and A. Sanyal, *Eur. Polym. J.*, 2021, **153**, 110514.
7 D. Ehrhardt, J. Mangialetto, J. Bertouille, K. Van Durme, B. Van Mele and N. Van den Brande, *Polymers*, 2020, **12**, 1–24.
8 N. Ten Brummelhuis, C. Diehl and H. Schlaad, *Macromolecules*, 2008, **41**, 9946–9947.
9 C. Liu, T. Li, J. Zhang, S. Chen, Z. Xu, A. Zhang and D. Zhang, *Prog. Org. Coat.*, 2016, **90**, 21–27.
10 M. Doura, Y. Naka, H. Aota and A. Matsumoto, *Macromolecules*, 2005, **38**, 5955–5963.
11 P. Mandal, S. Choudhury and N. K. Singha, *Polymer*, 2014, **55**, 5576–5583.
12 A. A. Kavitha, A. Choudhury and N. K. Singha, *Macromol. Symp.*, 2006, **240**, 232–237.
13 M. Destarac, *Macromol. React. Eng.*, 2010, **4**, 165–179.
14 K. Matyjaszewski, *Eur. Polym. J.*, 2024, **211**, 113001.
15 X. Pan, M. Fantin, F. Yuan and K. Matyjaszewski, *Chem. Soc. Rev.*, 2018, **47**, 5457–5490.
16 P. Krys and K. Matyjaszewski, *Eur. Polym. J.*, 2017, **89**, 482–523.
17 N. V. Tsarevsky and K. Matyjaszewski, *J. Polym. Sci., Part A:Polym. Chem.*, 2006, **44**, 5098–5112.
18 K. Matyjaszewski, W. Jakubowski, K. Min, W. Tang, J. Huang, W. A. Braunecker and N. V. Tsarevsky, *Proc. Natl. Acad. Sci. U. S. A.*, 2006, **103**, 15309–15314.
19 K. Matyjaszewski, *Adv. Mater.*, 2018, **30**, 1–22.
20 N. Chan, M. F. Cunningham and R. A. Hutchinson, *Macromol. Chem. Phys.*, 2008, **209**, 1797–1805.
21 M. Alrefai and M. Marić, *J. Polym. Sci.*, 2024, pol.20240466.
22 C. E. Hoyle and C. N. Bowman, *Angew. Chem., Int. Ed.*, 2010, **49**, 1540–1573.
23 M. Alrefai, V. Meola and M. Maric, *J. Polym. Sci.*, 2023, **61**, 289–303.
24 P. Shivapooja, L. K. Ista, H. E. Canavan and G. P. Lopez, *Biointerphases*, 2012, **7**, 1–9.
25 J. Sun, Y. Zhang, J. Li, Q. Ren, C. Wang and Z. Xu, *J. Macromol. Sci., Part A: Pure Appl. Chem.*, 2015, **52**, 609–616.
26 Z. Wang, H. Liang, H. Yang, L. Xiong, J. Zhou, S. Huang, C. Zhao, J. Zhong and X. Fan, *Prog. Org. Coat.*, 2019, **137**, 105282.
27 M. Fan, J. Liu, X. Li, J. Zhang and J. Cheng, *Ind. Eng. Chem. Res.*, 2014, **53**, 16156–16163.
28 X. Wang, K. Zhao, X. Huang, X. Ma and Y. Wei, *High Perform. Polym.*, 2019, **31**, 51–62.
29 F. Orozco, J. Li, U. Ezekiel, Z. Niyazov, L. Floyd, G. M. R. Lima, J. G. M. Winkelman, I. Moreno-Villoslada, F. Picchioni and R. K. Bose, *Eur. Polym. J.*, 2020, **135**, 109882.
30 P. Mandal and N. K. Singha, *RSC Adv.*, 2014, **4**, 5293–5299.
31 T. O. Machado, C. Sayer and P. H. H. Araujo, *Eur. Polym. J.*, 2017, **86**, 200–215.
32 S. M. Morozova, *Gels*, 2023, **9**, 102.

© 2025 The Author(s). Published by the Royal Society of Chemistry

Open Access Article. Published on 03 January 2025. Downloaded on 7/19/2025 8:17:25 PM.
This article is licensed under a Creative Commons Attribution-NonCommercial 3.0 Unported Licence.

33 E. E. L. Maassen, Dynamic covalent chemistry for UV curable networks, Phd thesis, Chemical Engineering and Chemistry, Technische Universiteit Eindhoven, 2019.
34 D. J. Hall, H. M. Van Den Berghe and A. P. Dove, *Polym. Int.*, 2011, **60**, 1149–1157.
35 C. Winkler, J. A. Rodriguez Agudo, U. Schwarz and M. Schäffler, *Adhes. Adhes. + Sealants*, 2021, **18**, 19–24.
36 E. P. Chang, *J. Adhes.*, 1997, **60**, 233–248.
37 I. Benedek, *Pressure-Sensitive Adhesives and Applications*, 2004.
38 T. G. Mezger, *The Rheology Handbook*, 2020.
39 C. Toncelli, D. C. De Reus, F. Picchioni and A. A. Broekhuis, *Macromol. Chem. Phys.*, 2012, **213**, 157–165.
40 P. Buono, A. Duval, L. Averous and Y. Habibi, *Polymer*, 2017, **133**, 78–88.
41 D. Ehrhardt, K. Van Durme, J. F. G. A. Jansen, B. Van Mele and N. Van den Brande, *Polymer*, 2020, **203**, 122762.

© 2025 The Author(s). Published by the Royal Society of Chemistry